Structural and Magnetic Properties of Fe2CrSi Heusler Alloy and Tunneling Magneto Resistance of its Magnetic Tunneling Junctions

Wang, Yu-Pu; Qiu, Jin-Jun; Lu, Hui; Yap, Qi-Jia; Wang, Wen-Hong; Han, Gu-Chang; Ngo, Duc-The; Teo, Kie-Leong

Publication date:
2013

Document Version
Publisher's PDF, also known as Version of record

Structural and Magnetic Properties of Fe_2CrSi Heusler Alloy and Tunneling MagnetoResistance of its Magnetic Tunneling Junctions

Yu-Pu Wang[1,2], Jin-Jun Qiu[2], Hui Lu[1], Qi-Jia Yap[2], Wen-Hong Wang[2], Gu-Chang Han[2], Duc-The Ngo[1], and Kie-Leong Teo[1]

[1]Department of Electrical and Computer Engineering, Advanced Memory Laboratory, National University of Singapore, 4 Engineering Drive 3, Singapore 117583

[2]Data Storage Institute, Agency for Science, Technology and Research (A*STAR), 5 Engineering Drive 1, Singapore 117608

wangyupu@nus.edu.sg

Abstract

We report the magnetic properties, microstructure and surface morphology of epitaxially grown Fe_2CrSi films. Highly ordered B2 films were obtained by deposition at room temperature followed by annealing at 400°C. Magnetic tunnel junctions using Fe_2CrSi show a tunnelling magnetoresistance (TMR) of 2.5%. The low TMR is ascribed to the oxidation of Fe_2CrSi at the interface with MgO. An enhancement of TMR to 8.1% was achieved by inserting a 0.3nm Mg between Fe_2CrSi and MgO to prevent the oxidation of Fe_2CrSi.

Keywords: Heusler alloy, half metal, MTJ, TMR, Fe_2CrSi

Introduction

The emerging field of spintronics exploits both the charge and spin properties of electrons to make devices more compact and faster. An important application in spintronics involves the injection of spin polarized current through a non-magnetic barrier layer, such as MgO barrier in magnetic tunnelling junctions (MTJs). The spin injection is low in the metal based spintronics device due to the mismatch of conductivity at the interface [1]. One possible solution to overcome the conductivity mismatch is to use half metallic ferromagnets (HMFs) with 100% spin polarization [2]. Categories of promising HMFs include Heusler alloys, oxide-based HMFs, perovskite manganites and zinc-blende HMFs. Among them, Heusler alloys have the greatest potential to realize half metallicity at room temperature due to their lattice constant matching with the III-V semiconductors, high Curie temperature (>400 K) and large bandgap at Fermi level [3]. Many research groups have focused on investigating Co-based Heusler alloys, such as Co_2MnSi, Co_2MnAl, and Co_2CrAl [4-8]. An alternative candidate for HMF is Fe-based Heusler alloy, such as Fe_2CrSi (FCS). FCS is predicted to be a half metal in the $L2_1$ structure [9]. Compared with other Heusler alloys, FCS possesses the following advantages [9,10]: Firstly, the calculated majority DOS of FCS at Fermi level is as high as 7.0 states/eV, which is about 5 times higher than that of Co_2MnSi, leading to a high spin polarization; Secondly, the magnetization of FCS is found to be small (~2 μ_B/f.u.), in contrast to that of the Co-based Heusler alloy (4-6 μ_B/f.u.) [4-9], allowing for a low critical current for spin transfer torque switching in spin torque devices [11]; Thirdly, FCS has a suitable Curie temperature of 630K, which is low enough for thermally assisted recording, yet high enough compared to room temperature.

The FCS film was reported to be obtained in B2 structure instead of $L2_1$ structure due to its structural instability [9]. However, according to theoretical studies, FCS in B2 structure is also expected to show high spin-polarization [12-14]. The same group also attempted to utilize FCS films in a magnetic tunnelling junction (MTJ) structure [9], but no TMR was reported, probably due to a rough surface of the FCS layer and a resultant strong coupling between the free layer and the pinned layer. Hence, a high-quality MTJ involving FCS has yet to be achieved.

In this paper, we focus on the implementation of B2 phase FCS thin film in MTJ structure. Highly-ordered FCS in B2 structure has been successfully grown by magnetron sputtering, and exhibits excellent magnetic properties and surface roughness (RMS~0.18 nm) for application in MTJ structures. The tunnel magnetoresistance (TMR) ratio and the resistance-area product (RA) of the barrier MgO layer were measured by the current-in-plane-technique (CIPT) on un-patterned MTJ samples. TMR ratio and RA were studied as a function of post-annealing temperature. It is found that a well-defined exchange bias is established for our MTJ samples and a TMR ratio of 2.5% is obtained at room temperature in the MTJ sample with a 1.5 nm MgO barrier. This TMR ratio is greatly enhanced to 8.1% with an insertion of Mg layer between FCS and MgO barrier that could prevent the oxidation of the bottom electrode FCS layer.

Experimental Procedure

All samples were prepared by ultra high vacuum magnetron sputtering system with a base pressure of 5×10^{-10} Torr. The FCS thin films were grown by the sputtering of a stoichiometric $Fe_{46}Cr_{30}Si_{24}$ target and were deposited at room temperature on MgO (100) substrates with Cr and Ag buffer layers. Prior to any deposition, the MgO substrate was optimized by pre-heating at 600°C for 1 hour. *In-situ* thermal treatments for the FCS layer were performed at various temperatures of 300°C, 400°C, and 500°C for 15 minutes to form ordered structure. After optimizing the FCS films, MTJs with a stacking structure of MgO(100)/Cr 40nm/FCS 30nm/MgO t nm/CoFe 5nm/IrMn 12nm/Ru 8nm were fabricated subsequently. The MgO barriers were grown by RF sputtering in a plasma oxidation chamber. A barrier MgO thickness of 1.5 nm was used to obtain a reasonable RA for CIPT measurements. Furthermore, an Mg layer was inserted between FCS and MgO barrier layer which is expected to enhance the TMR ratio. During the deposition of the stack, a

978-1-4673-4842-3/13/$31.00

series of *in-situ* thermal treatments were done as follows: 700°C for Cr buffer layer for 30 minutes; 400°C for FCS thin film for 15 minutes. All these samples were naturally cooled to room temperature in vacuum. The whole junctions were then *ex-situ* post-annealed at various temperatures from 200°C to 500°C in high vacuum in the presence of an in-plane magnetic field of 1 Tesla.

Vibrating sample magnetometer (VSM) and alternating gradient magnetometer (AGM) were used to characterize the magnetic properties. X-ray diffraction (XRD) and transmission electron microscopy (TEM) were employed to characterize the crystalline structure. The surface roughness was investigated using atomic force microscope (AFM). TMR ratio and RA of the MTJs were measured by CIPT on un-patterned samples.

Results and Discussions

Fig. 1(a) shows the XRD (θ-2θ) patterns for MgO (100)/Cr/Ag/FCS samples under various thermal treatment conditions. When the *in-situ* annealing temperature is 400°C and above, FCS (200) and (400) peaks are clearly observed, indicating the formation of highly ordered B2 structure. However, the intensity of these peaks becomes weaker when the annealing temperature increases to 500°C. AFM measurements indicate that smooth films were obtained when the annealing temperature is below 500°C. The best surface roughness of 0.18 nm is obtained at an annealed temperature of 400°C as shown in Fig. 1(b), whereas the surface of the sample annealed at 500°C becomes rough with particles protruding from the surface clearly observed, as shown in Fig. 1(c). These artifacts are somehow similar to that reported previously [9] in which the film was deposited at high temperatures that led to a rough surface. As shown in Fig. 1(d), the rocking curve of FCS(400) of the film *in-situ* annealed at 400°C shows a narrow peak with the full width at half maximum (FWHM) as small as 0.53°, in contrast to 1.3° reported in the literature [9]. These results indicate that the FCS film was grown in the highly ordered B2 structure with the c-axis perpendicular to the plane. The optimized condition for the FCS films in terms of surface roughness and crystalline structure is obtained when the *in-situ* annealing temperature is 400°C. Cross-sectional TEM image for the film is illustrated in Fig. 1(e). The image clearly shows that the smooth and abrupt interfaces are formed between the layers in the structure of MgO substrate/Cr/Ag/FCS. The high resolution TEM image in Fig. 1(f) as well as the fast Fourier transform (FFT) image [inset of Fig. 1(f)] confirms that the deposited FCS layer is single crystalline.

Fig. 2 depicts *M-H* loop for the FCS thin film with *in-situ* annealing at 400°C. The field was applied along the in-plane [011] direction, which is parallel to the easy axis of the crystalline anisotropy of FCS. Sharp magnetization reversal is observed and the ratio of remnant magnetization (M_r) over saturation magnetization (M_S) is about 1, reflecting the easy-axis is along [011] direction. The M_S and coercivity (H_C) of FCS are 322 emu/cc and 2.2 Oe, respectively. The M_S of FCS is relatively smaller than that of Co_2MnSi, Co_2FeSi, and Co_2FeAl bulk (1000-1200 emu/cc), which is favourable for the low switching current density required for spin-transfer torque devices, such as STT-MRAM [11]. FCS with small H_C is also a suitable ferromagnetic material for soft magnetic electrodes in MTJ applications.

MTJs with stacking structure of MgO substrate/Cr 40nm/FCS 30nm/MgO 1.5nm/CoFe 5nm/IrMn 8nm/Ru 3nm were fabricated. We examined the post-annealing effect with temperatures ranging from 200°C to 500°C. Fig. 3(a) shows the XRD (θ-2θ) patterns for MTJs fabricated under different post-annealing temperatures. The FCS(200), Cr(200), and FCS(400) peaks are clearly observed, indicating that our samples are (100) orientation of epitaxial growth. Even without any post-annealing for the MTJ, clear FCS(200) and FCS(400) peaks are observed, indicating that (100)-orientated highly ordered B2 structure of FCS was already formed during *in-situ* annealing. When the post-annealing temperature increases to 200°C, the intensity of FCS(400) peak remains the same but that of FCS(200) peak becomes weaker. When the post-annealing temperature raises to 300°C, the FCS(400) peak is still quite strong but the FCS(200) peak disappears, which indicates poorer crystalline structure of FCS. When the post-annealing temperature further increases to 350°C, the FCS(400) peak becomes weaker in addition to the disappearance of the FCS(200) peak, showing that the crystalline structure of FCS becomes even more deteriorated. We ascribed the deterioration of the crystalline structure after post-annealing to possible oxidation of FCS during annealing. Fig. 3(b) presents the M_S and H_C of FCS as a function of post-annealing temperature. The M_S obtained is as high as 360 emu/cc under 200°C post-annealing, which is close to the calculated M_S for FCS with an $L2_1$ ordered structure (398 emu/cc) [15]. Band calculation predicted that the half metallicity of FCS is robust against most defects (e.g., antisites, swaps, and vacancies) [16]. Hence, the presented FCS with a B2 order and 360 emu/cc M_S is expected to have a high spin polarization. The increase in M_S can be attributed to the improvement of the chemical order and local stoichiometry after thermal treatment. The decrease in H_C with annealing temperature reveals possible reduction in defect density accompanied with an enhancement of crystalline quality. However, the annealing at higher temperatures results in lower M_S of FCS, which is suspected to be related to a migration of oxygen from the MgO barrier layer into FCS layer. In other words, oxidation of the underlying FCS ferromagnetic layer suppresses the total magnetic moment of the FCS film.

Fig. 4(a) shows the room temperature *M-H* loop of the MTJs post-annealed at different temperatures measured by AGM. An exchange bias is observed with 200°C post-annealing. However, the H_C of the top CoFe electrode is quite large, which indicates CoFe is not well pinned by the antiferromagnetic IrMn layer due to low post-annealing temperature. When the post-annealing temperature increases to 350°C, as shown from the *M-H* loop in Fig. 4(a), a well-defined exchange bias between the top CoFe and IrMn is established and H_C of the CoFe layer reduces significantly. The M_S of the FCS free layer and the CoFe pinned layer are 322 emu/cc and 1102 emu/cc, respectively. This indicates that FCS layer and CoFe layer with a highly ordered structure are obtained in the MTJ structures. It is worthwhile to note that the *M-H* loop of the free layer and pinned layer in our MTJ samples post-annealed at 350°C are well-separated with a shift of 220 Oe. The exchange bias in *M-H* loop of MTJ structure we obtained is better-defined than that reported previously [9]. However, when the post-annealing temperature is above 500°C, the exchange bias is destroyed and the magnetization of two

magnetic layers switches simultaneously, resulting in no TMR effect. The vanishing of the exchange bias in this case could be attributed to the diffusion of the Mn from IrMn to the other layers. The post-annealing temperature dependence of RA and TMR ratio of these samples are shown in Fig. 4(b). The highest TMR ratio (2.5 %) measured by CIPT on un-patterned samples is achieved for the sample annealed at 200°C. The annealing of the MTJs at an appropriate temperature improves not only the structural properties of the upper electrode but also the interfacial structural properties, leading to an enhancement of the TMR ratios [17-20]. As seen in Fig. 4(b), TMR ratio decreases with the post-annealing temperature above 200°C, although the exchange bias is well developed. This decrease in TMR ratio is highly likely due to the oxidation of FCS layer [21, 22] at the interface with the MgO barrier. The oxidized FCS surface may act as additional scattering centres for spin polarized tunnelling electrons, which would suppress TMR. The oxidation of FCS at the interface is further confirmed from the monotonically increasing RA with increase in post-annealing temperature. The TMR ratio and RA relationship is illustrated in the inset of Fig. 4(a). The highest TMR ratio is obtained with RA of 2000 ohm/μm^2. The decrease in TMR ratio at higher RA values is probably because of the polarization reduction of the FCS layer due to the oxidation. We propose that the FCS surface is considered oxidized because it was exposed to oxygen during MgO deposition, and more serious oxidation of FCS occurs as the post-annealing temperature is increased. In order to avoid the FCS oxidation, a 0.3 nm Mg layer was inserted between the FCS layer and the barrier MgO layer to enhance the TMR effect. Since the Mg layer will be oxidized eventually forming MgO, the thickness of the MgO layer is now reduced to 1.2 nm to retain the total thickness of the tunnelling barrier (Mg+MgO) as 1.5 nm. An enhancement of the TMR ratio up to ~8.1% is obtained apparently when the sample is annealed at 250°C. However, this TMR ratio is still lower than the expected from the first-principle calculations [23]. As shown in Ref. [9], DOS profile of the majority spin of FCS at Fermi level is very sharp and close to the conduction band edge. Hence, the DOS profile would be easily affected by thermal fluctuations and imperfections of FCS crystalline structure. As a result, a little shift of the Fermi level may cause a large reduction of the DOS of the majority spin, resulting in low spin polarization and TMR ratio. Therefore, the tuning of the Femi level would be critical to obtain high TMR ratio when using FCS as an electrode in MTJ structure.

Conclusion

In summary, this study investigated magnetic tunnel junctions with an (100)-epitaxial FCS bottom electrode and MgO tunnel barrier. The epitaxial FCS showed very low surface-roughness (RMS~0.18nm) and highly ordered B2 structure. The plasma oxidation process of the MgO tunnel barrier may have caused oxidation of the bottom FCS surface. Oxidation of the bottom electrode interface increased the RA value and reduced TMR ratio. With 1.5nm MgO tunnel barrier, a TMR ratio of 2.5% was obtained. This TMR ratio is suppressed by bottom electrode oxidation. Insertion of Mg layer between bottom electrode and MgO tunnel barrier helped to enhance the TMR ratio to 8.1% by protecting the FCS layer from the oxidation. Optimization of FCS electrode (e.g., adjustment of Fermi level of FCS, interfacial studies) is expected to engender higher and more stable spin polarization and enhanced TMR ratios.

References

[1] Mark Johnson, and R. H. Silsbee, Phys. Rev. Lett. 55, 17, pp. 1790-1793 (1985).
[2] R. A. de Groot and F. M. Mueller, Phys. Rev. Lett. 50, 25, pp. 2024-2027 (1983).
[3] J. Dubowik, I. Goscianska, A. Szlaferek, Y. V. Kudryavtsev, Mater. Sci. Poland 25, 2 (2007).
[4] K. Yakushiji, K. Saito, S. Mitani, K. Takanashi, Y. K. Takahashi, and K. Miyazaki, and H. Kubota, Appl. Phys. Lett. 88, 192508 (2006).
[5] Y. Sakuraba, M. Hattori, M. Oogane, Y. Ando, H. Kato, A. Sakuma, T. Hono, Appl. Phys. Lett. 88, 222504 (2006).
[6] S. Ishida, S. Fujii, S. Kashiwagi, and S. Asano, J. Phys. Soc. Jpn. 64, 2152 (1995).
[7] I. Galanakis, P. H. Dederiches, and N. Papanikolaou, Phys. Rev. B 66,174429 (2002).
[8] S. Picozzi, A. Continenza, and A. J. Freeman, Phys. Rev. B 66, 094421 (2002).
[9] S. Yoshimura, H. Asano, Y. Nakamura, K. Yamaji, Y. Takeda, M. Matsui,S. Ishida, Y. Nozaki, and K. Matsuyama, J. Appl. Phys. 103, 07D716 (2008).
[10] V. Ko, J. Qiu, P. Luo, G.C. Han, and Y.P. Feng, J. Appl. Phys. 109, 07B103 (2011).
[11] S. Mangin, Y. Henry, D. Ravelosona, J. A. Katine, and Eric E. Fullerton, Appl. Phys. Lett. 94, 012502 (2009).
[12] S. Ishida, S. Mizutani, S. Fujii, and S. Asano, Mater. Trans. 47, 31 (2006).
[13] S. Ishida, S. Mizutani, S. Fujii, and S. Asano, Mater. Trans**.** 47, 464 (2006).
[14] S. Mizutani, S. Ishida, S. Fujii, and S. Asano: Mater. Trans. 47, 25 (2006).
[15] H. Sukegawa, H. Xiu, O. Ohkubo, T. Furubayasi, T. Niizeki, W. Wang, S. Kasai, S. Mitani, K. Inomata, and K. Hono, Appl. Phys. Lett. 96, 212505 (2010).
[16] B. A. Hamad, Eur. Phys. J. B 80, 11-18 (2011).
[17] T. Ishikawa, S. Hakamata, K.-i. Matsuda, T. Uemura, and M. Yamamoto:J. Appl. Phys. 103, 07A919 (2008).
[18] T. Ishikawa, H. Liu, T. Taira, K.-i. Matsuda, T. Uemura, and M.Yamamoto: Appl. Phys. Lett. 95, 232512 (2009).
[19] M. Yamamoto, T. Ishikawa, T. Taira, G. Li, K.-i. Matsuda, and T. Uemura:J. Phys.: Condens. Matter 22 , 164212 (2010).
[20] S. Tsunegi, Y. Sakuraba, M. Oogane, K. Takanashi, and Y. Ando: Appl.Phys. Lett. 93, 112506 (2008).
[21] Y. Sakuraba, J. Nakata, M. Oogane, Y. Ando, H. Kato et al., Appl. Phys. Lett. 88,022503 (2006).
[22] Sungjun Joo, K. Y. Jung, B. C. Lee, Tae-Suk, Kim, K. H. Shin et al., Appl. Phys. Lett. 100,172406 (2012).
[23] Shinpei Fujii, Shoji Ishida, and Setsuro Asano, J. Phys. Soc. Jap 81, 034716 (2012).

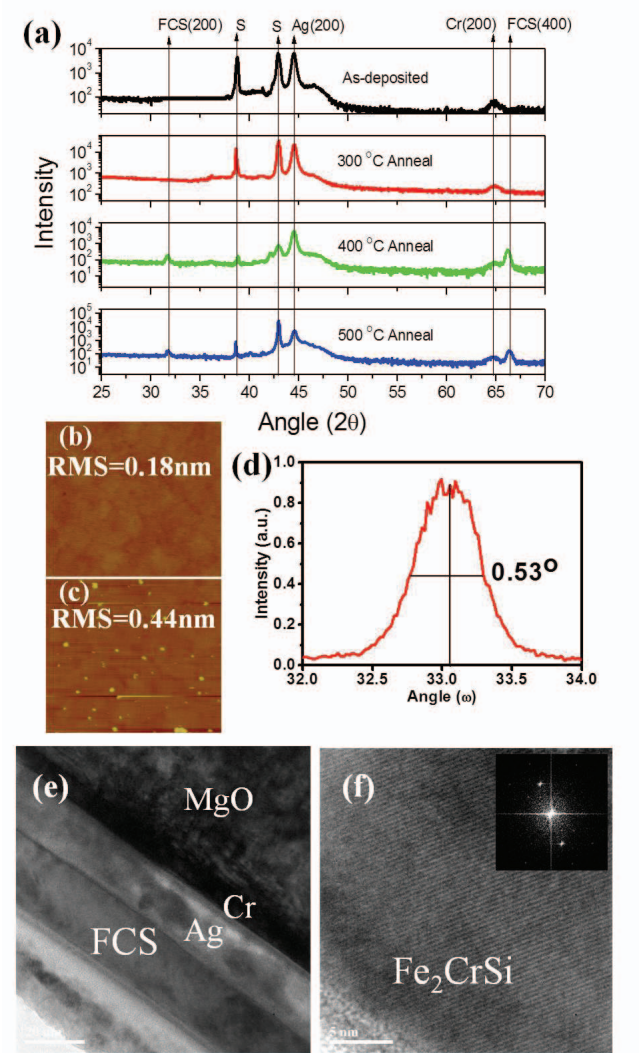

Fig. 1 (a) X-ray Diffraction patterns for Fe_2CrSi thin film. From top to bottom, *in-situ* annealing are as deposited, 300°C, 400°C, and 500°C, respectively. S refers to substrate peak from K_α and K_β, respectively. (b) AFM image of Fe_2CrSi thin film with 400°C, and (c) 500°C *in-situ* annealing. (d) Rocking curve measurement of Fe_2CrSi(400) peak. (e) TEM image of MgO/Cr/Ag/ Fe_2CrSi sample. (f) High resolution TEM of Fe_2CrSi thin film. The inset shows FFT image of the Fe_2CrSi layer.

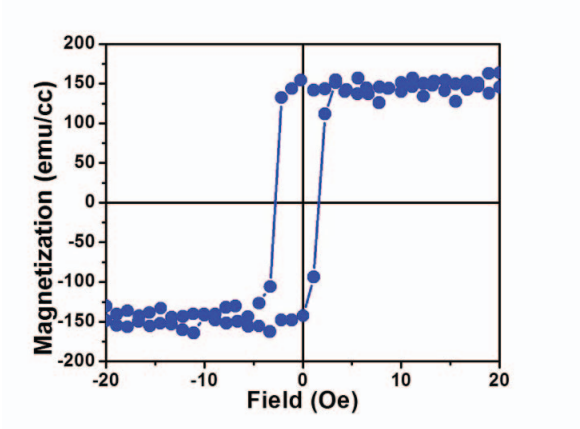

Fig. 2 *M-H* loop of Fe_2CrSi film with 400°C *in-situ* annealing along [011] direction using VSM.

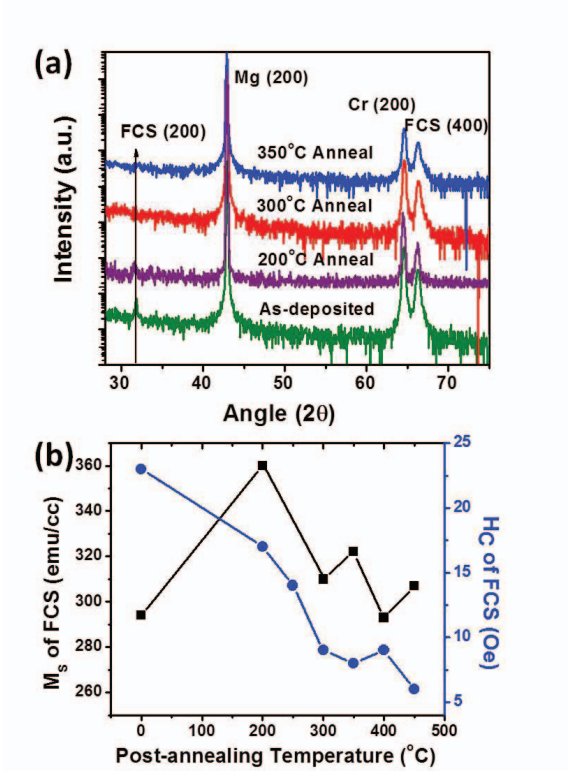

Fig. 3 (a) X-ray Diffraction patterns for MTJs. From bottom to top, post-annealing are as deposited, 200°C, 300°C, and 350°C, respectively. (b) M_S and H_C of the bottom electrode Fe_2CrSi for MTJs, as a function of post-annealing temperature.

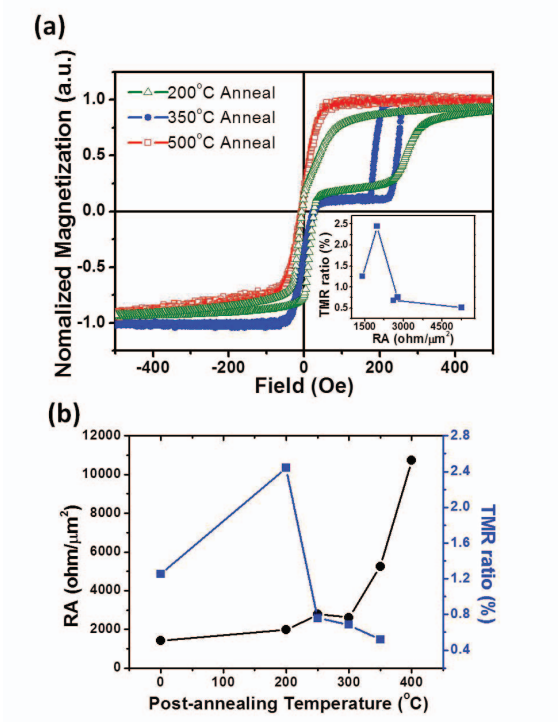

Fig. 4 (a) *M-H* loop for MTJs with 200°C, 350°C, and 500°C post-annealing, respectively. The inset figure is TMR ratio as a function of Resistance-Area. (b) Resistance-Area production and TMR ratio as a function of post-annealing temperature.